Supporting Information

for

Mild Redox Complementation Enables H_2 Activation by [FeFe]-Hydrogenase Models

James M. Camara and Thomas B. Rauchfuss*

Corresponding Author: rauchfuz@illinois.edu

I. Experimental Procedures

II. Tables

Table S1. Observed pseudo-first-order rate constants for reaction of $[Fe_2(adt^{Bn})(dppv)(PMe_3)(CO)_3][BAr^F{}_4]$ with H_2 at 0 °C in the presence of $P(o\text{-}tol)_3$ and $[Me_8Fc]BAr^F{}_4$ at varying $[H_2]$ in CD_2Cl_2. $[Fe_2]_o$ = 4.67 mM, $[P(o\text{-}tol)_3]_o$ = 4.67 mM, $[Fc^+]_o$ = 4.67 mM.

III. Figures

Figure S1: ^2H NMR spectrum (97 MHz, CD_2Cl_2) of reaction $[Fe_2(adt^{Bn})(dppv)(PMe_3)(CO)_3]BAr^F{}_4$ with D_2 of $P(o\text{-}tol)_3$ and $[Me_8Fc]BAr^F{}_4$, showing ^2H incorporation into the product hydride and phosphonium.

Figure S2: Plot of k_{obs} vs $[H_2]$ for the reaction of $[Fe_2(adt^{Bn})(dppv)(PMe_3)(CO)_3]BAr^F{}_4$ with H_2 at 0 °C in the presence of $P(o\text{-}tol)_3$ and $[Me_8Fc]BAr^F{}_4$ at varying $[H_2]$. $[Fe_2]_o$ = 4.67 mM, $[P(o\text{-}tol)_3]_o$ = 4.67 mM, $[Fc^+]_o$ = 4.67 mM.

Figure S3: Cyclic voltammogram of **2**. Conditions: 1.0 mM [**2**], 100 mM $[Bu_4N]PF_6$, CH_2Cl_2, 20 °C, 0.1 V/s scan rate, referenced to Fc/Fc^+, i_{pa}/i_{pc} = 1.06

Figure S4. Representative kinetic plot with first-order fit. Inset: linearized first-order plot for the appearance of product. $[\mathbf{1}^+]_o$ = 4.67 mM, $[P(o\text{-}tol)_3]_o$ = 4.67 mM, $[Me_8Fc^+]_o$ = 14 mM, 0 °C.

Figure S5: UV-Vis of the reaction of [**2**]BAr^F_4 with H_2 (1atm) at 20 °C in the presence of [Fc][BAr^F_4]. Inset: normalized cross sections at 405 nm and 550 nm.

Figure S6: Plot for estimation of pseudo-first-order rate constant for activation of H_2 (1800 psig) by [$\mathbf{1}^+$] in toluene at room temperature *without additional oxidant present* from the data in ref 1.

IV. Calculations

A. Estimation of rate enhancement of H_2 activation by [2^+]/[Fc][BAr^F_4].

B. Calculation of inverse KIE for H_2 binding to $Ir(H)_2Cl(P^tBu_2Me)_2$ from reported data.

I. Experimental Procedures

All procedures were carried out using standard Schlenk Techniques. All solvents were dried and degassed by passage through activated alumina and sparging with argon respectively. IR spectra were recorded on a Perkin Elmer Spectrum 100. Cyclic voltammetry was performed under nitrogen on a BAS CV-50W potentiostat, with glassy carbon working electrode, Pt wire counter electrode and Ag/Ag^+ reference. ^1H and ^{31}P NMR spectra were recorded on a Varian Unity 500 MHz NMR Spectrometer. ^2H NMR spectra were acquired on a Varian Unity 600 MHz spectrometer equipped with an autoX probe. X-band EPR spectra were collected on a Varian E-122 spectrometer. $Fe_2[(SCH_2)_2NBn](CO)_6$,[1] $Fe_2[(SCH_2)_2NBn](dppv)(PMe_3)(CO)_3$,[2] and $[Fe_2(SCH_2CH_2S)(PMe_3)_2(CO)_4]PF_6$ were prepared according to published procedures.[2]

$Fe_2([(SCH_2)_2NBn])(dppn)(CO)_4$, 2. Into a flask outfitted with a reflux condenser under slow argon purge was added $Fe_2[(SCH_2)_2NBn](CO)_6$ (500 mg, 1.05 mmol), dppn (520 mg, 1.05 mmol) and 50 mL toluene. The solution was refluxed for 22 h. Toluene was removed under vacuum, the remaining solid was washed with pentane (2 x 20 mL), and the product dried under vacuum. Yield = 0.71g (73%). ^{31}P NMR (500 MHz, C_6D_6, 20°C): δ 68.3 (s); ^1H NMR (500 MHz, C_6D_6, 20°C): δ 7.95-6.65 (m, 31H), 2.82 (s, 2H), 2.66 (d, J_{H-H} = 6 Hz, 2H), 2.45 (d, J_{H-H} = 6 Hz, 2H). IR (CH_2Cl_2): ν_{CO} = 2021 (s), 1949 (m), 1913 (w) cm^{-1}. Anal. Calcd for $C_{47}H_{37}Fe_2NO_4P_2S_2$ (found): C, 61.52 (61.89); H, 4.06 (4.13); N 1.53 (1.63).

$[Fe_2[(SCH_2)_2NBn](dppn)(CO)_4]BAr^F_4$, $[2]BAr^F_4$. To a Schlenk flask containing $Fe_2[(SCH_2)_2NBn](dppn)(CO)_4$ (100mg, 1.09 mmol) and $[Fc]BAr^F_4$ (114 mg, 1.09 mmol) was added 15 mL of CH_2Cl_2 at -78°C, generating a deep purple solution. To the cooled flask was added hexanes (30 mL), resulting in partial precipitation of the product $[\mathbf{2}]BAr^F_4$. The flask was evacuated at -78°C until the purple product precipitated fully, leaving an orange solution. The orange solution was removed by filter cannula, and the product washed with cold hexanes (10 mL) and dried under vacuum. Yield: 1.55 g (77%). IR(CH_2Cl_2): ν_{CO} = 2078 (s), 2022 (m), 1896 (w) cm^{-1}. Single crystals were obtained by layering 20 mL pentane onto 5 mL of 22 mM $[\mathbf{2}]^+/CH_2Cl_2$ solution under argon. EPR samples were prepared in 1:1 CH_2Cl_2/Toluene, and were 1 mM in $[2]BAr^F_4$.

General Procedure for Generation of $[HFe_2[(SCH_2)_2NBn](dppv)(PMe_3)(CO)_3]BAr^F_4$, $[1H]BAr^F_4$, via H_2 with varying oxidants. A J. Young tube was charged with $Fe_2[(SCH_2)_2NBn](dppv)(PMe_3)(CO)_3$ (3mg, 3.5 μmol), P(o-tol)$_3$ (1 mg, 3.5 μmol), oxidant (7.0 μmol), and $[HFe_2(SCH_2CH_2S)(PMe_3)_2(CO)_4]PF_6$ (2.1 mg, 3.4 μmol) as internal standard. To the tube was added 0.75 mL of CD_2Cl_2. The tube was then evacuated, pressurized with 2 atm H_2, shaken, and cooled to 0 °C. Spectroscopic properties (^1H NMR, ^{31}P NMR, and IR) of the products matched those previously reported.[2] The reaction was monitored by appearance of the product hydride peak at (δ -15.38, t, J_{P-H} = 21Hz) in the ^1H NMR. Spectra were acquired for at least 3 half-lives, and with an acquisition time of 4.1 s, and a delay time of 5 s to ensure accurate integrations. Oxidants tested were $[Me_{10}Fc]BAr^F_4$ (8.2 mg, 7.0 μmol) and (16.4 mg, 14 μmol), $[Me_8Fc]BAr^F_4$ (8 mg, 7.0 μmol) and (16 mg, 14 μmol), and $[Cp^*FcCp]BAr^F_4$ (7.8 mg, 7.0 μmol). Data were imported to Origin V8.1 and fit to first order exponentials. Reported rate constants are averages of multiple runs. Kinetic data are in Table 1. A representative kinetic plot with first-order fit is shown in Figure S4.

$[DFe_2[(SCH_2)_2NBn)(dppv)(PMe_3)(CO)_3]BAr^F_4$ via D_2 and $[Me_{10}Fc]BAr^F_4$. A J. Young tube was charged with $Fe_2[(SCH_2)_2NBn)](dppv)(PMe_3)(CO)_3$ (3 mg, 3.5 μmol), P(o-tol)$_3$

(1 mg, 3.5 μmol), $[Me_{10}Fc]BAr^F_4$ (8.2 mg, 7.0 μmol), and 0.75 mL of CH_2Cl_2. The tube was evacuated and pressurized with 2 atm D_2, and allowed to react at 0 °C overnight. The ^2H NMR spectrum is shown in Figure S1.

General Procedure for kinetic measurement of H_2 dependence. Samples were prepared as above using $Fe_2[(SCH_2)_2NBn](dppv)(PMe_3)(CO)_3$ (3 mg, 3.5 μmol), $P(o\text{-}tol)_3$ (1 mg, 3.5 μmol), $[Me_8Fc]BAr^F_4$ (8 mg, 7.0 μmol), and $[HFe_2(SCH_2CH_2S)(PMe_3)_2(CO)_4]PF_6$ (2.1 mg, 3.4 μmol) as internal standard. After addition of 0.75 mL of CD_2Cl_2, the samples were frozen, evacuated, and filled with the appropriate amount of H_2. Samples were initially pressurized with 1, 2, and 3 atm of H_2. Because the samples were pressurized while cold, the pressure inside the tube increased upon thawing. Therefore, the concentration of H_2 was determined from the final spectrum by integration of the H_2 resonance at δ4.6 vs the internal standard. The H_2 resonance was observable throughout the entire reaction. The total acquisition and delay time were suitable for integration of the H_2 signal.[3] The measured concentrations of H_2 were consistent with reported literature values.[4] Progress of reaction was determined by the integration of the product $[HFe_2[(SCH_2)_2NBn](dppv)(PMe_3)(CO)_3]^+$ (δ -15.38, t, $J_{P\text{-}H}$ = 21 Hz) vs that of the standard. Data were imported to Origin V8.1 and fit to first order exponentials. The data are in Table S1 and a plot of k_{obs} vs $[H_2]$ is in Figure S2.

$[HFe_2[(SCH_2)_2N(H)Bn])(dppn)(CO)_4][BAr^F_4]_2$ via H_2 and $[Fc]BAr^F_4$. In a Schlenk flask $Fe_2([(SCH_2)_2NBn])(dppn)(CO)_4$ (9.6 mg, 10.5 μmol) was dissolved in 3 mL of CH_2Cl_2. A solution of $[Fc][BAr^F_4]$ (21.0 μmol) in 1.0 mL of CH_2Cl_2 was added to the flask, resulting in an immediate color change to deep purple. H_2 was bubbled through the solution, and the reaction was monitored by IR. The solution underwent a color change from purple to yellow-orange within minutes. The initial IR(CH_2Cl_2) ν_{CO} bands (2078 (s), 2022 (m), 1896 (w) cm^{-1}) disappeared with concomitant growth of new bands at (2043 (s), 1986 (m), 1971 (m), 1932 (w) cm^{-1}) corresponding to $[HFe_2([(SCH_2)_2N(H)Bn])(dppn)(CO)_4][BAr^F_4]_2$ (Figure 3). ^1H NMR (500 MHz, CD_2Cl_2, 20°C): δ -13.85 (t, $J_{P\text{-}H}$ = 15 Hz), -13.91 (d, $J_{P\text{-}H}$ = 19 Hz).

$[HFe_2([(SCH_2)_2N(H)Bn])(dppn)(CO)_4][BAr^F_4]_2$ via $[H(OEt_2)_2][BAr^F_4]$ and $Fe_2([(SCH_2)_2NBn])(dppn)(CO)_4$. To a Schlenk flask was added $Fe_2([(SCH_2)_2NBn])(dppn)(CO)_4$ (5mg, 5.5 μmol) and 3 mL of CH_2Cl_2. A 1 mL solution of $[H(OEt_2)_2]BAr^F_4$ (12 mg, 10.9 μmol) was added to the flask. The solution showed an immediate color change from brown to yellow-orange. IR(CH_2Cl_2): ν_{CO} = 2043 (s), 1986 (m), 1971 (m), 1932 (w) cm^{-1}. ^1H NMR (500 MHz, CD_2Cl_2, 20 °C): δ -13.85 (t, $J_{P\text{-}H}$ = 15 Hz), -13.91 (d, $J_{P\text{-}H}$ = 19 Hz).

Kinetics of formation of $[HFe_2([(SCH_2)_2N(H)Bn])(dppn)(CO)_4][BAr^F_4]_2$ via H_2 and $[Fc]BAr^F_4$. A J. Young tube was charged with $Fe_2[(SCH_2)_2NBn](dppn)(CO)_4$ (3.2 mg, 3.5 μmol) and $[Fc]BAr^F_4$ (7.0 μmol). To the tube was added 0.75 mL of CD_2Cl_2. The tube was then evacuated, pressurized with 2 atm H_2, shaken, and inserted into the NMR spectrometer (pre-cooled to 0 °C). The reaction was monitored by appearance of the product isomeric hydrides at δ -13.75 to -14.0 in the ^1H NMR spectrum vs the residual solvent peak at δ5.32. Spectra were acquired with an acquisition time of 4.1 s, and a delay time of 5 s to ensure accurate integrations. Data were imported to Origin V8.1 and fit to first-order exponentials, yielding an observed first order rate constant of $k_{obs} = 4.8(3) \times 10^{-4}\ s^{-1}$.

Isotope effect for activation of H_2 by $[Fe_2[(SCH_2)_2NBn](dppn)(CO)_4]BAr^F_4$ in the presence of $[Fc]BAr^F_4$. A stock solution was prepared by addition of $Fe_2[(SCH_2)_2NBn](dppn)(CO)_4$ (5 mg, 5.45 μmol) and $[Fc]BAr^F_4$ (11.25 mg, 10.9 μmol) to a

Schlenk flask and addition of 27 mL of CH_2Cl_2, resulting in a purple solution. Into a Schlenk cuvette was transferred 2 mL of the solution. The solution was frozen, the cuvette evacuated and back filled with 1 atm of H_2 (or D_2). The solution was thawed, and the reaction progress was monitored by UV-vis spectroscopy at a constant temperature of 20 °C. The UV-vis spectra showed disappearance of the starting material band at 550 nm and appearance of a new band at 405 nm, with isosbestic points at 380 and 502 nm (Figure S5). The data were exported into SpecFit/32 (ref), and the data fit to a first order equation using global analysis. Experiments were performed in triplicate. The measured isotope effect was $k_H/k_D = (9.0(7) \times 10^{-4)}/(1.2(1) \times 10^{-3}) = 0.75(8)$.

II. Tables

Table S1. Observed pseudo-first-order rate constants for reaction of $[Fe_2(adt^{Bn})(dppv)(PMe_3)(CO)_3]BAr^F{}_4$ with H_2 at 0 °C in the presence of $P(o\text{-tol})_3$ and $[Me_8Fc]BAr^F{}_4$ at varying $[H_2]$ in CD_2Cl_2. $[Fe_2]_o = 4.67$ mM, $[P(o\text{-tol})_3]_o = 4.67$ mM, $[Fc^+]_o = 4.67$ mM.

Initial H_2 pressure (atm)	$[H_2]$ (M)	k_{obs} (s^{-1}) x 10^5
1	0.005	2.4(2)
2	0.017	4.2(5)
3	0.022	5.0(2)

III. Figures

Figure S1: ^{2}H NMR (97 MHz, CD_2Cl_2) spectra of the reaction $[Fe_2(adt^{Bn})(dppv)(PMe_3)(CO)_3]BAr^F{}_4$ with D_2 of $P(o\text{-}tol)_3$ and $[Me_8Fc]BAr^F{}_4$ showing formation of $[DFe_2(adt^{Bn})(dppv)(PMe_3)(CO)_3]^+$ and $DP(o\text{-}tol)_3{}^+$.

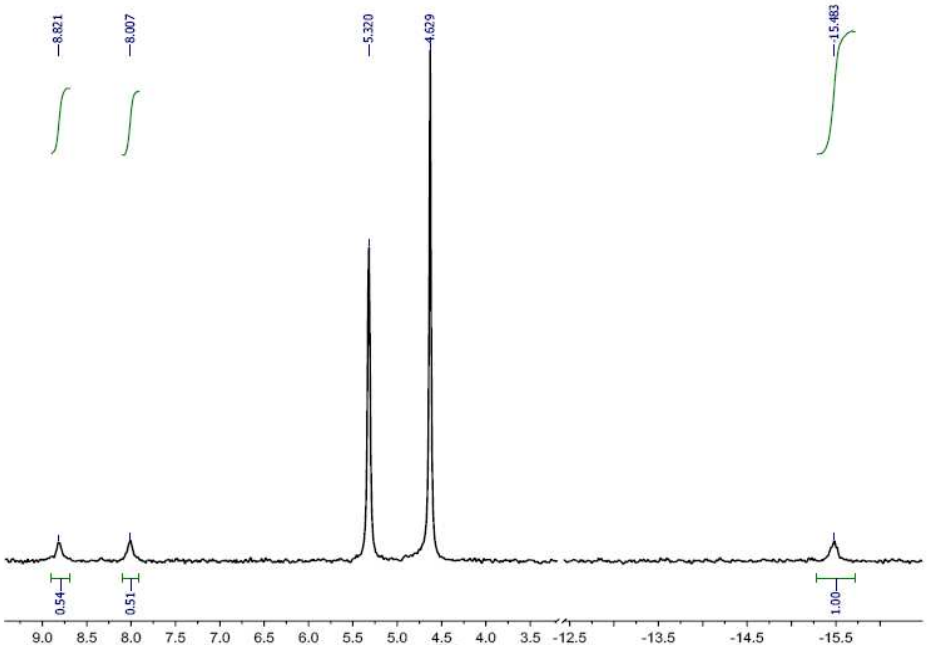

Figure S2: Plot of k_{obs} vs $[H_2]$ for the reaction of $[Fe_2(adt^{Bn})(dppv)(PMe_3)(CO)_3]BAr^F{}_4$ with H_2 at 0 °C in the presence of $P(o\text{-}tol)_3$ and $[Me_8Fc]BAr^F{}_4$ at varying $[H_2]$. $[Fe_2]_o = 4.67$ mM, $[P(o\text{-}tol)_3]_o = [Fc^+]_o = 4.67$ mM.

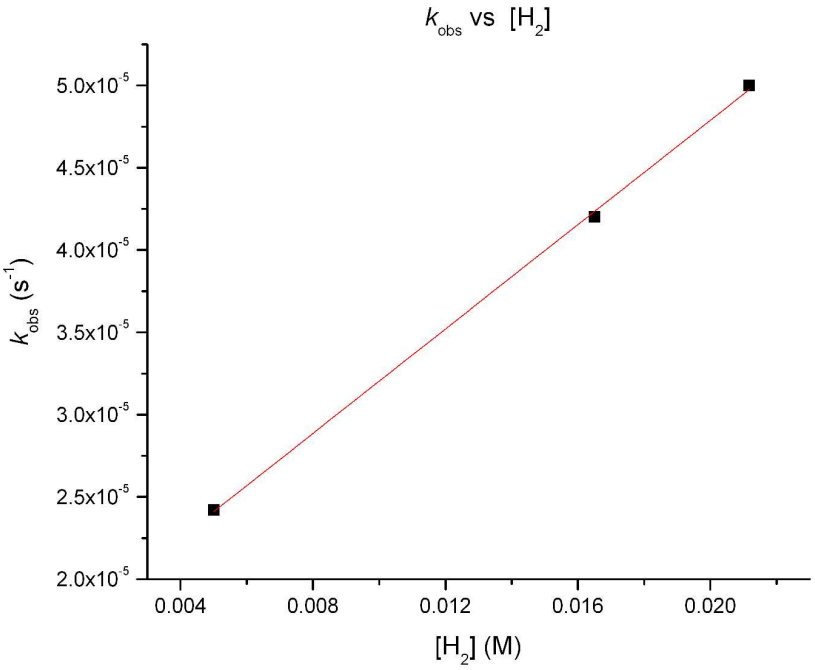

Figure S3. Cyclic voltammogram of **2**. Conditions: 1.0 mM [**2**], 100 mM $[Bu_4N]PF_6$ in CH_2Cl_2, 25 °C, 0.1 V/s scan rate, referenced to Fc/Fc^+. Results: $i_{pa}/i_{pc} = 1.06$, $E_{1/2} = -254$ mV.

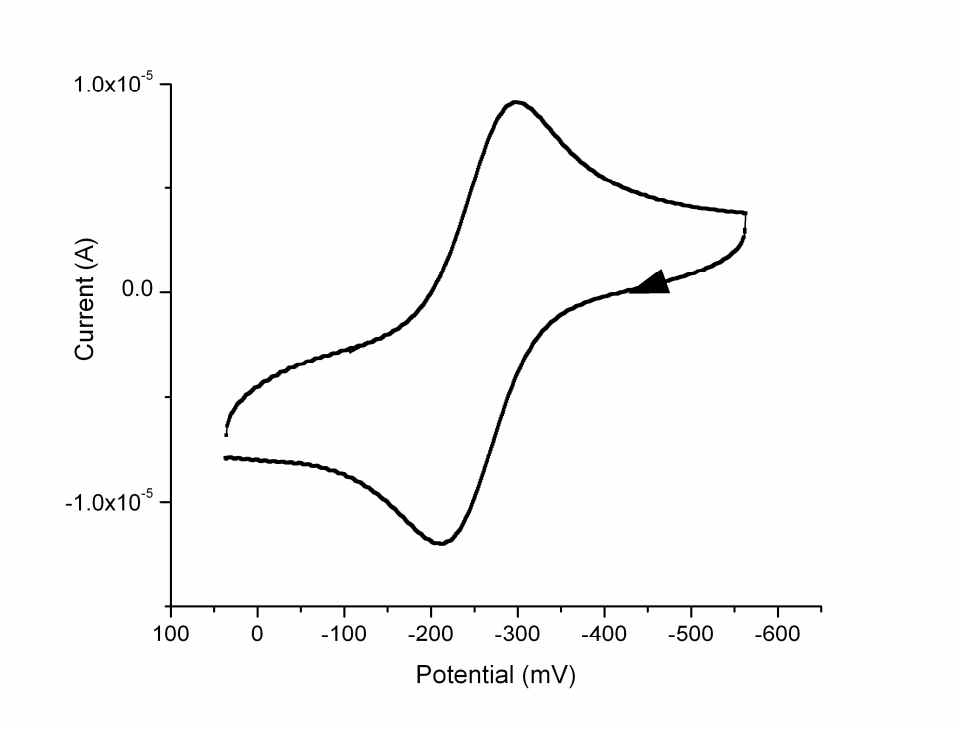

Figure S4. Representative kinetic plot with first-order fit. Inset: linearized first-order plot for the appearance of product. $[\mathbf{1}^+]_o$ = 4.67 mM, $[P(o\text{-tol})_3]_o$ = 4.67 mM, $[Me_8Fc^+]_o$ = 14 mM, 0 °C.

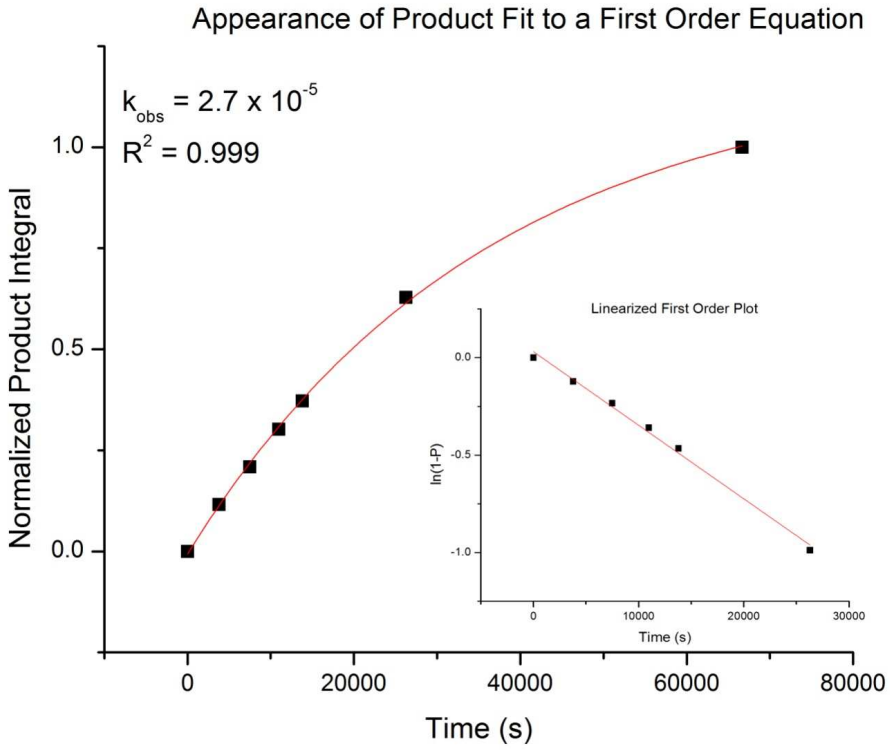

Figure S5: UV-Vis of the reaction of [**2**]BAr^F_4 with H_2 (1atm) at 20 °C in the presence of [Fc][BAr^F_4]. Inset: normalized cross sections at 405 nm and 550 nm.

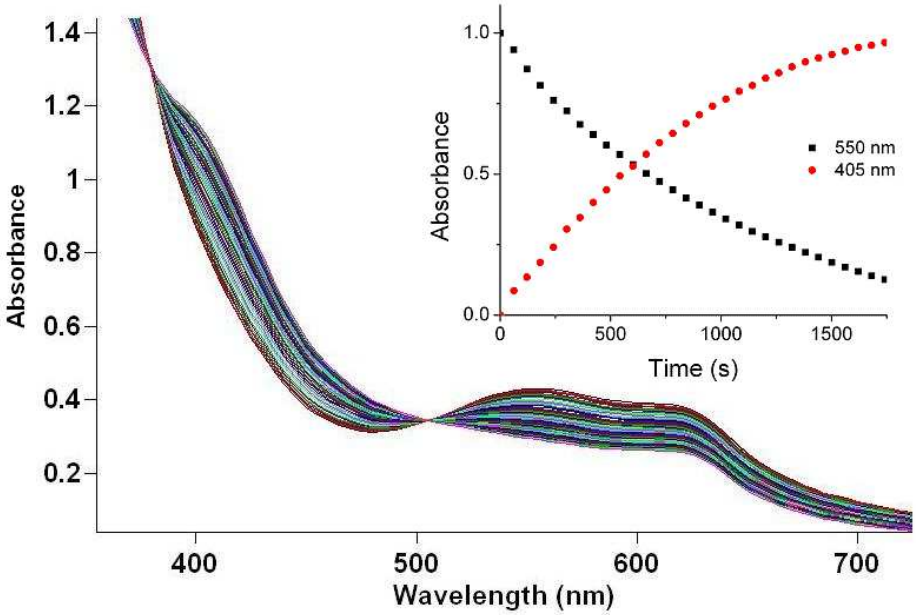

Figure S6. Plot for estimation of pseudo-first-order rate constant for activation of H_2 (1800 psig) by $[\mathbf{1}]^+$ in toluene at room temperature *without additional oxidant present* from the data in ref 1.

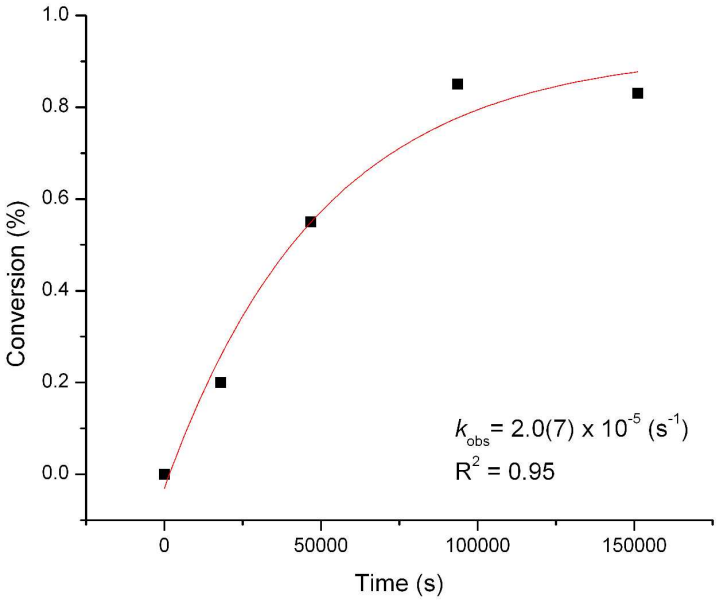

IV. Calculations

A. Estimation of rate enhancement of H_2 activation by $[2^+]/[Fc]BAr^F_4$.

The supporting information of our previous study[2] contains conversion vs time data for the reaction of $[\mathbf{1}^+]$ with 1800 psig H_2 in toluene, at room temperature, and *without additional oxidant present*. Assuming analogous kinetics to those measured for $[\mathbf{1}]^+$, (first order in $[H_2]$ and $[Fe_2]$, H_2 dissolves more quickly than it is consumed), a pseudo-first-order rate constant can be calculated from the half-life, or from a plot of conversion vs time (Figure S6).

$$k_{obs} = k[H_2] \approx 2 \times 10^{-5}\ (s^{-1})$$

The concentration of $[H_2]$ in solution can be estimated from the reported solubility (given as mole fraction) of H_2 in toluene at 29 °C.[5]

$$\chi \approx 0.16 \quad \Rightarrow \quad [H_2] \approx 1.8\ M$$

Dividing the estimated k_{obs} by $[H_2]$ yields a second order rate constant, adjusted for $[H_2]$.

$$k \approx \frac{k_{obs}}{[H_2]} \approx \frac{2 \times 10^{-5}\ s^{-1}}{1.8\ M} \approx 1 \times 10^{-5}\ M^{-1}s^{-1}$$

The observed pseudo-first-order rate constant for activation of H_2 by $[\mathbf{2}]^+$ in the presence of $[Fc]BAr^F_4$ at 1 atm H_2 and 20 °C (see isotope effect measurements) can be converted to the corresponding second order rate constant analogously. From the reported solubility[4] of H_2 in CH_2Cl_2 at 20 °C ($\chi = 1.86 \times 10^{-4}$), the concentration $[H_2]$ is 3 mM. The corresponding second order rate constant is given by:

$$k' \approx \frac{k_{obs}}{[H_2]} \approx \frac{9 \times 10^{-4}\ s^{-1}}{0.003\ M} \approx 3 \times 10^{-1}\ M^{-1}s^{-1}$$

The ratio of the two second order rate constants k'/k shows a rate enhancement of 10^4.

B. Calculation of inverse KIE for H_2 binding to $Ir(H)_2Cl(P^tBu_2Me)_2$ from reported data.[6]

Caulton and coworkers report a normal kinetic isotope effect for H_2 dissociation from $(H)_2Ir(H)_2Cl(P^tBu_2Me)_2$ at 20 °C in toluene.

$$Ir(H)_2Cl(P^tBu_2Me)_2 + \mathbf{H_2} \underset{k^H_{-1}}{\overset{k^H_1}{\rightleftharpoons}} (\mathbf{H_2})Ir(H)_2Cl(P^tBu_2Me)_2 \quad \vdots \quad \frac{k^H_{-1}}{k^D_{-1}} = 1.8$$

The equilibrium constants for the dissociation of H_2 from $(H)_2Ir(H)_2Cl(P^tBu_2Me)_2$, and D_2 from $(D_2)Ir(D)_2Cl(P^tBu_2Me)_2$ in toluene over temperatures ranging from 250-294 °K are also reported.

Though the values are only reported in the plot of figure 7, the ΔH^o and ΔS^o values derived from the plot allow straightforward calculation of the corresponding equilibrium constants.

$$Ir(H)_2Cl(P^tBu_2Me)_2 + \mathbf{H_2} \underset{k^H_{-1}}{\overset{k^H_1}{\rightleftharpoons}} (\mathbf{H_2})Ir(H)_2Cl(P^tBu_2Me)_2 \quad K^H_{diss} = \frac{k^H_{-1}}{k^H_1} = .133\ M$$

$$Ir(H)_2Cl(P^tBu_2Me)_2 + \mathbf{D_2} \underset{k^D_{-1}}{\overset{k^D_1}{\rightleftharpoons}} (\mathbf{D_2})Ir(H)_2Cl(P^tBu_2Me)_2 \quad K^D_{diss} = \frac{k^D_{-1}}{k^D_1} = .062\ M$$

The kinetic isotope for binding of H_2 is given thus given by:

$$\frac{k^H_1}{k^D_1} = \left(\frac{k^H_{-1}}{k^D_{-1}}\right)\left(\frac{K^D_{diss}}{K^H_{diss}}\right) = (1.8)(0.466) = 0.84$$

(1) Li, H.; Rauchfuss, T. B. *J. Am. Chem. Soc.* **2002**, *124*, 726-727.
(2) Olsen, M. T.; Barton, B. E.; Rauchfuss, T. B. *Inorganic Chemistry* **2009**, *48*, 7507-7509.
(3) Sartori, E.; Ruzzi, M.; Turro, N. J.; Decatur, J. D.; Doetschman, D. C.; Lawler, R. G.; Buchachenko, A. L.; Murata, Y.; Komatsu, K. *J. Am. Chem. Soc.* **2006**, *128*, 14752-14753.
(4) Shirono, K.; Morimatsu, T.; Takemura, F. *J. Chem. & Eng. Data* **2008**, *53*, 1867-1871.
(5) Simnick, J. J.; Sebastian, H. M.; Lin, H.-M.; Chao, K.-C. *J. Chem. & Eng. Data* **1978**, *23*, 339-340.
(6) Hauger, B. E.; Gusev, D.; Caulton, K. G. *J. Am. Chem. Soc.* **1994**, *116*, 208-214.